CHARACTERIZATION OF DIFFERENT WC-Co CEMENTED-CARBIDE TOOLS

KARAKTERIZACIJA ORODIJ IZDELANIH IZ RAZLIČNIH WC-Co KARBIDNIH TRDIN

Iztok Naglič[1*], Adam Zaky[1], Blaž Leskovar[1], Miha Čekada[2], Boštjan Markoli[1]

[1]University of Ljubljana, Faculty of Natural Sciences and Engineering, Ljubljana, Slovenia
[2]Jožef Stefan Institute, Department of Thin Films and Surfaces, Ljubljana, Slovenia

This paper deals with the characterization of three different commercial, WC-Co cemented-carbide tools in the form of saw blades, one group of which exhibits more frequent cracking. Since the properties of these materials largely depend on the microstructure, a detailed characterization was carried out using scanning electron microscopy (SEM), energy-dispersive X-ray spectroscopy (EDS) and X-ray diffraction (XRD). The SEM image analysis included a determination of the binder content and the mean WC grain area. The average chemical composition of these materials was also determined using an X-ray fluorescence (XRF) analyser. The results show that despite the same content of binder-forming elements in all three WC-Co cemented-carbide materials, the material that cracked more frequently contained a smaller amount of binder and a lower mean WC grain area, both of which are known to reduce the toughness of such a material.

Keywords: microstructure, WC-Co cemented carbide, scanning electron microscopy, X-ray diffraction

Prispevek obravnava karakterizacijo treh orodij v obliki žaginih listov izdelanih iz različnih komercialnih WC-Co karbidnih trdin, od katerih ena skupina pogosteje poka. Ker so lastnosti teh materialov v veliki meri odvisne od mikrostrukture, je bila podrobna karakterizacija izvedena z uporabo vrstične elektronske mikroskopije (SEM), energijsko disperzijske rentgenske spektroskopije (EDS) in rentgenske difrakcije (XRD). Analiza SEM slik je vključevala določanje vsebnosti veziva in povprečne površine WC zrn. Z rentgenskim fluorescenčnim (XRF) analizatorjem smo določili tudi povprečno kemično sestavo teh materialov. Rezultati kažejo, da je kljub enaki vsebnosti elementov, ki tvorijo vezivo, v vseh treh materialih pogosteje pokala karbidna trdina, ki je vsebovala manjši delež veziva in manjšo povprečno površino WC zrn. Znano je, da oba parametra zmanjšujeta žilavost takšnega materiala.

Ključne besede: mikrostruktura, WC-Co karbidna trdina, vrstična elektronska mikroskopija, rentgenska difrakcija

1 INTRODUCTION

WC-Co cemented carbides are an important tool material that has been known for nearly 100 years. These materials are widely used in manufacturing industry due to their excellent combination of hardness, toughness and thermal conductivity.[1,2] WC-Co cemented carbides consist of a hard hexagonal WC phase with high thermal conductivity and a face-centred cubic (fcc) cobalt binder phase. The binder phase is the minority phase in these materials. Cobalt is the most used binder metal in cemented carbides due to its excellent wettability of WC and its mechanical properties. In addition to cobalt, nickel, iron and their combinations are also used as binders in various proportions in certain applications.[1,3–5] Pure cobalt exhibits a hexagonal structure at temperatures up to 417 °C, while the fcc structure is stable above that. After sintering is complete, the binder cools and the fcc structure is retained. This can be attributed to the dissolution of tungsten in cobalt and the higher thermal expansion of cobalt compared to WC. After cooling, the binder phase remains loaded with tensile stress.[1] Alloying elements such as Ni, which has infinite solid solubility with Co, also stabilises the fcc structure.[6]

The microstructure of cemented carbides is of great importance as it affects the properties of these materials. Therefore, by adjusting the binder content and the WC grain size, the mechanical properties such as toughness, hardness and thermal conductivity can be adjusted.[1,2,7] It has been reported that WC-Co cemented-carbide wear increases with increasing cobalt content and WC grain size.[8] The microstructures of these materials have been described by many authors with different quantities and relationships between them. These quantities are WC grain size, carbide contiguity, volume fraction of the binder, and binder mean free path, and many of them are more-or-less obviously related to each other.[1] Carbide contiguity is a quantity that measures the amount of WC/WC contacts. Various models relate it to the volume fraction of the binder and the WC grain size. In contrast, the binder mean free path is related to the average WC grain size and the volume fraction of the binder, which in turn is proportional to the cobalt content. Consequently, most of the properties of these materials can be described by simply relating them to the cobalt or binder content and the WC grain size. The correlations between

these two quantities and the main properties of these materials are well established and can be explained by simple correlations. A higher thermal conductivity is obtained by a larger WC grain size and a low binder content, while a high hardness is obtained by a small WC grain size and a low binder content. On the other hand, high toughness can be achieved by a large WC grain size and a high binder content, while high edge toughness is achieved by a small WC grain size and a high binder content.[1,2,7]

Several elements were found to inhibit the grain growth of WC grains during the sintering process. These elements are vanadium, titanium, chromium, tantalum, molybdenum and niobium. In addition to the grain size, these inhibitors also affect the shape of the grains.[9,10] It has been reported that the grain-growth inhibitors act by forming a thin cubic (M,W)C layer on the surface of the WC grains, which lowers the interfacial energy and acts as a kinetic barrier.[3,11–13] Chromium additions have also been found to increase the corrosion resistance of WC-Co cemented carbides.[14]

Carbon content must be controlled during the manufacturing process of cemented carbides. A low carbon content leads to the formation of η-phase, which are ternary carbides composed of carbon, cobalt and tungsten. The M_6C carbides can range from Co_3W_3C to Co_2W_4C, while $M_{12}C$ has a fixed composition of Co_6W_6C. The presence of relatively large amounts of the brittle η-phase leads to a degradation in the mechanical properties of these carbides.[1,2,15] First-principles calculations of the elastic modulus and hardness of η-phases revealed that they have lower elastic moduli than WC and are significantly softer than WC and W_2C.[16] On the other hand, a high carbon content during the manufacturing process leads to the formation of graphite precipitates, which degrade the mechanical properties.

Three different commercial WC-Co cemented-carbide tool materials were used as saw blades. Cracking of

tools occurred more frequently in the saw blades made from one group of materials than in the other two. It is well known that the microstructure of these materials strongly affects the mechanical properties. Therefore, in this work we performed the characterization of the microstructure of these three different commercially available WC-Co carbide materials to find the most probable cause of this frequent cracking.

2 EXPERIMENTAL PART

We characterized the microstructure of three different commercial WC-Co cemented-carbide tool materials, shaped as saw blades with a diameter of 35 mm and a thickness of 0.4 mm. These different materials were designated as sample 1, sample 2, and sample 3. Cracking occurred more frequently in the tools made from the sample 3 material than in the tools made from samples 1 and 2. Smaller pieces of the tools were mounted, ground, and polished. Final polishing was performed with 0.25-µm diamond paste.

The average chemical composition of the tool materials was determined using the Thermo Scientific Niton XL3t GOLDD+ X-ray fluorescence (XRF) analyser. Scanning electron microscopy (SEM) at (8, 15 and 20) kV was performed using ThermoFisher Scientific Quattro S equipped with Oxford Ultim Max EDS detectors for energy dispersive X-ray spectroscopy (EDS) and JEOL JSM 7600F equipped with Oxford Instruments INCA Microanalysis Suite and X-Max 20 SDD-EDS detector. X-ray diffraction (XRD) was used to characterise the phases present in these materials. X-ray diffraction patterns were recorded with a PANalytical X'Pert PRO diffractometer using non-monochromatic X-rays generated by Empyrean Cu anode tube.

The microstructural analysis also included the determination of the volume fraction of a binder in the samples. The content of the binder phase was determined us-
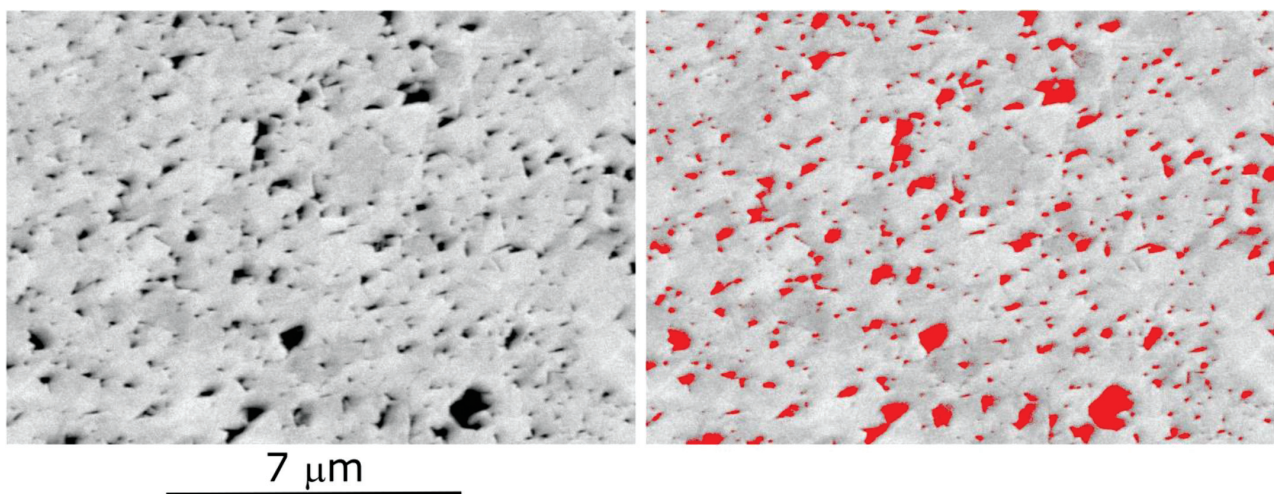

Figure 1: Backscattered-electron image of the microstructure of sample 2 for the determination of the binder content and the same image with red-coloured detected binder phase

Table 1: Chemical composition of the tool materials, determined with XRF (*w*/%)

	W	Co	Cr	Ni	Co + Ni
Sample 1	96.34 ± 0.44	3.58 ± 0.08	0.09 ± 0.09	–	–
Sample 2	96.00 ± 0.44	3.84 ± 0.09	0.16 ± 0.06	–	–
Sample 3	95.81 ± 0.46	2.90 ± 0.08	0.40 ± 0.07	0.89 ± 0.06	3.79 ± 0.14

ing backscattered-electron images taken with SEM at 8 kV, showing a large contrast between the light WC grains and the dark binder phase. The volume fraction was determined according to ASTM 1245-03 (2016) by image analysis of six to twelve backscattered-electron images using ImageJ 1.53f51 software. **Figure 1** shows the determination of the binder content of sample 2. The detected binder phase is coloured red.

To determine the size of WC grains, which also affects the mechanical properties of WC-Co cemented-carbide materials, the mean grain area was measured on backscattered-electron images taken at 15 kV using SEM. The mean grain area was determined according to ASTM E1382-97 by the grain count (planimetric) method using AxioVision software on six images of the microstructure of each sample. The grain area of a region with many grains was outlined and measured. This grain

Figure 2: Backscattered-electron image of the microstructure with example for the determination of the mean grain area by grain count (planimetric) method: a) sample 2, b) sample 3

area was then reduced by the volume fraction of the binder phase and divided by the number of grains. **Figure 2** presents an example of the measurement of the mean grain area in samples 2 and 3 using the grain count (planimetric) method.

3 RESULTS AND DISCUSSION

The chemical composition, excluding the carbon content, of all three samples was determined by XRF. These results are presented in **Table 1**. The results show that all three samples contain tungsten, cobalt and chromium, while sample 3 also contains some nickel. These results indicate that the binder phase of samples 1 and 2 is mainly cobalt with traces of chromium, while the binder of sample 3 contains some nickel. Chromium is normally added as Cr_3C_2. Metallic chromium on the other hand, is soluble in cobalt. The chromium content in the samples is rather low. Therefore, if it is present in solid solution, it cannot significantly affect the mechanical properties by changing the content of the binder phase in these three samples. Nickel exhibits infinite solid solubility in cobalt.[6] Since the content of binder significantly affects the mechanical properties, it is crucial to determine the amount of binder in the studied samples. A comparison of the cobalt content shows that it is the highest in sample 2 and the lowest in sample 3, which was the most prone to cracking. Consequently, the content of binder-forming elements (cobalt and nickel) in sample 3 is 3.79 *w*/%, which is between samples 1 and 2. This is inconsistent with the fact that sample 3 was the one that cracked more frequently. We therefore performed an additional analysis to determine the volume fraction of the binder phase and the mean grain area via SEM images.

BE images of the microstructure of all three carbide tool materials are shown in **Figure 3.** The light phase represents the WC phase, while the dark area between the WC crystals is the cobalt-based binder phase. A comparison of the microstructures shows that the size of the WC crystals is smaller and the binder phase content is lowest in sample 3. The mechanical properties of such materials are affected by these two parameters. These two observations were analysed in more detail by determining the average volume fraction of the binder phase and the mean grain area of the WC phase using backscattered-electron images of the microstructure.

The contents of the binder phase determined by the analysis of the backscattered-electron images are listed in **Table 2**.
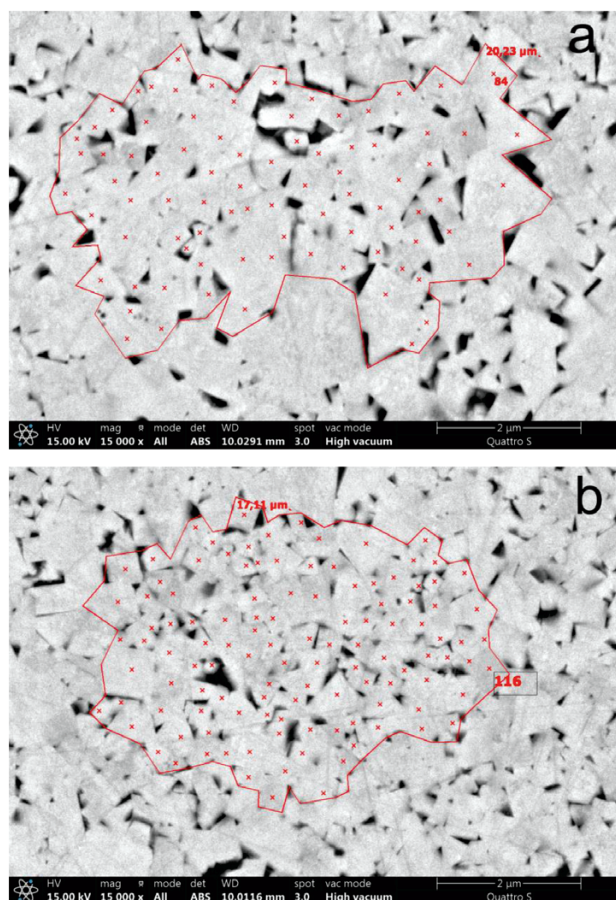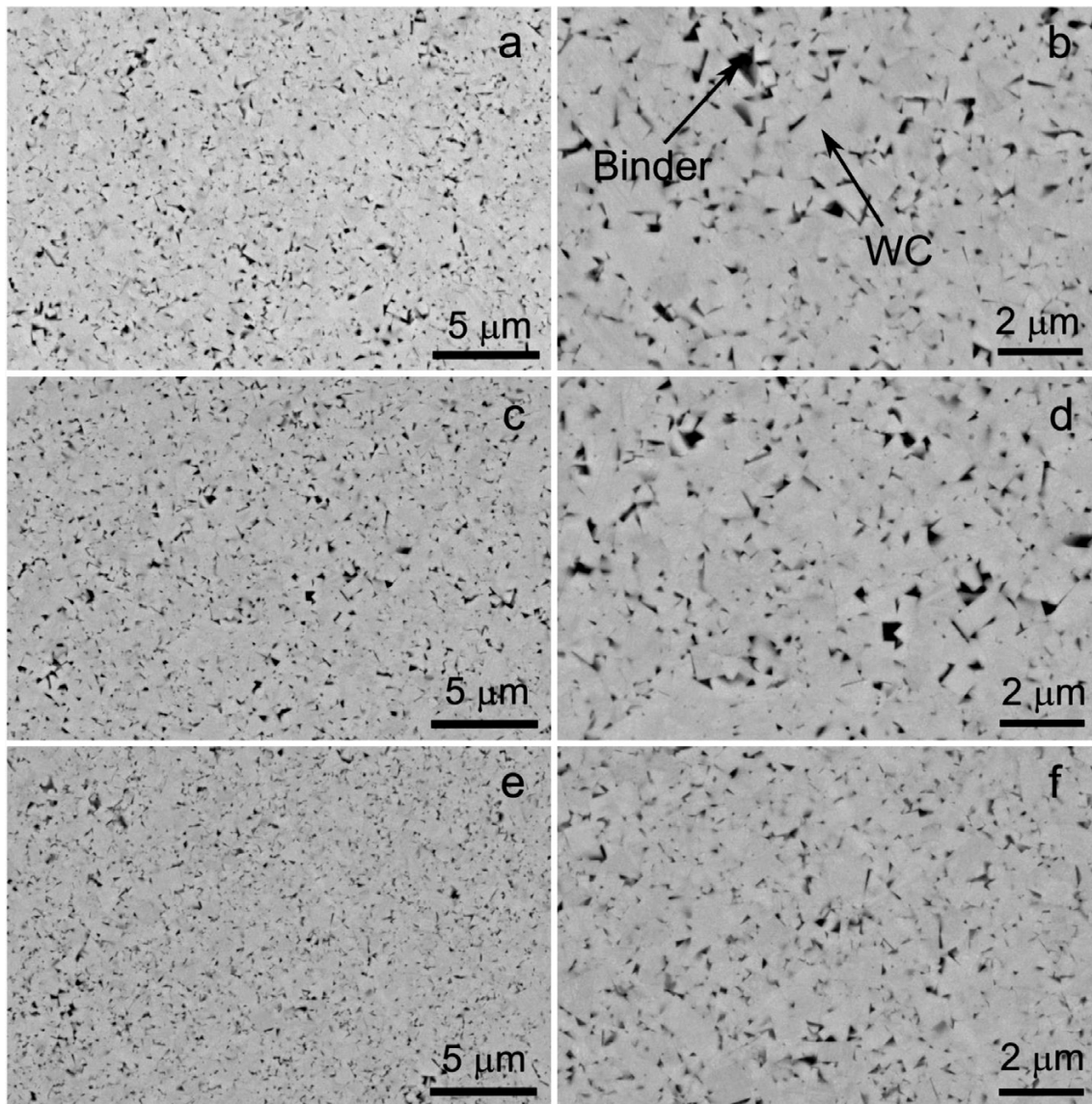
Figure 3: Backscattered-electron images of the microstructure of: a and b) sample 1, c and d) sample 2, e and f) sample 3

Table 2: Analysis of the backscattered-electron images

	Sample 1	Sample 2	Sample 3
Average volume fraction of binder (V_V)	0.0616	0.0600	0.0433
Standard deviation (s)	0.0067	0.0086	0.0061
95% confidence interval (95 % CI)	0.0062	0.0091	0.0039
Relative accuracy (% RA)	10.0	15.1	8.9

The results in **Table 2** show that the average volume fractions of the binder phase V_V in samples 1 and 2 are 0.0616 and 0.0600, respectively, while in sample 3 it is only 0.0433. Considering the standard deviation (s), the 95 % confidence interval (95 % CI), and the relative accuracy (% RA), it can be observed that the interval of $V_V \pm 95$ % CI of sample 3 does not overlap with samples 1 and 2, which means that the average volume fraction of binder in sample 3 is lower than in samples 1 and 2. This finding contradicts the previous result of the XRF analysis, which indicates that the content of the binder-form-

ing elements (cobalt and nickel) is similar to the cobalt content in samples 1 and 2. The lower content of binder in sample 3 ultimately leads to a lower toughness of this material and more frequent cracking.

Table 3 shows the results of the evaluation of the mean grain area of WC crystals. The mean grain area results confirm the observation of the microstructures in **Figure 1,** where the mean grain area is lowest for sample 3 with 0.139 μm², while these values are 0.246 μm² and 0.262 μm² for samples 1 and 2, respectively. Considering s, 95 % CI and % RA, it can be observed that the interval

of $\overline{A} \pm 95\%$ CI of sample 3 does not overlap with the intervals of samples 1 and 2, which means that the mean grain area of the WC crystals in sample 3 is smaller than in samples 1 and 2. This result is consistent with the result of the XRF analysis that the chromium content in sample 3 is significantly higher. Chromium is known to inhibit the grain growth and thus affects the final size of the WC grains. Nevertheless, it was not clear what role the nickel in sample 3 played or whether it had incorporated into the Co-based fcc binder phase and thus contributed to the total amount of binder.

Table 3: Results of the evaluation of the mean grain area of WC crystals

	Sample 1	Sample 2	Sample 3
Mean grain area of WC $\overline{A}$ (μm^2)	0.246	0.262	0.139
Standard deviation s (μm^2)	0.036	0.034	0.013
95% confidence interval (95 % CI (μm^2))	0.038	0.036	0.013
Relative accuracy (% RA)	15.6	13.6	9.7
Interval of mean grain area ($\overline{A} \pm 95\%$ CI (μm^2))	0.208 – 0.284	0.226 – 0.298	0.125 – 0.152

We therefore also performed EDS analyses of the binder phase. The analyses were performed on the largest area of binder in the microstructure of each sample. The EDS analyses of the binder phase are listed in **Table 4**. A low oxygen content is present only in sample 1, likely due to contamination. Carbon is present in all three samples, due in part to impurities and detection of the main phase in these samples, the WC phase. The tungsten content was the highest of all the elements detected in all three samples. Chromium, known to be an inhibitor of grain growth, is also present in all three samples, although its content is significantly higher in sample 3. This result is consistent with the XRF analysis presented in **Table 1** and the finding that the WC crystals are the smallest in this sample. Consequently, the binder phase in samples 1 and 2 consists mainly of cobalt, while sample 3 also contains a significant amount of nickel, as XRF analysis also shows. Assuming that only cobalt and nickel are present in the binder phase, the nickel content would be 22.6 $w/\%$.

To resolve our doubts, we also performed detailed XRD analyses to reveal the actual phases present in the microstructure of the three WC-Co cemented-carbide tools. The XRD patterns of all three samples are shown in **Figure 4**. The XRD patterns show that all three samples contain more-or-less the same phases, among which the hexagonal WC dominates (COD 9007456). The
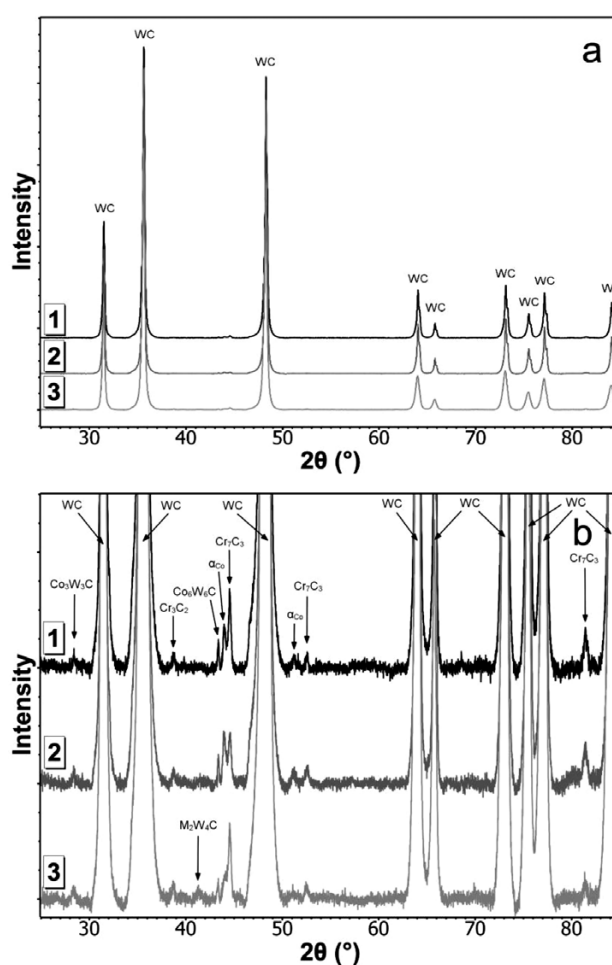

Figure 4: XRD patterns of samples 1, 2 and 3: a) unmagnified, b) magnified

binder phase α_{Co} (COD 9012949) with an fcc structure is also present. It is worth noting that the intensity of the two peaks for the binder phase α_{Co} in sample 3 is significantly lower than in the samples 1 and 2. This result indicates that sample 3 contains less binder phase than the other two samples and is consistent with the result obtained by determining the volume fraction of binder phase using backscattered-electron image analysis. In addition to the two previously mentioned phases, Co_6W_6C (ICCD 00-022-0597), Co_3W_3C (ICDD 00-006-0639), Cr_7C_3 (COD 1009019) and Cr_3C_2 (COD 9009906) are also present in all three samples.

The content of cobalt in samples 1 and 2 and of cobalt and nickel in sample 3 is similar, as shown in **Table 1**. On the other hand, the content of the binder, based on image analysis and XRD results, is clearly lower in

Table 4: EDS compositional analysis of a binder phase at 20 kV ($w/\%$)

	C	O	Cr	Co	Ni	W
Sample 1	9.2 ± 0.5	2.0 ± 0.2	0.8± 0.1	42.4 ± 0.4	–	45.6 ± 0.5
Sample 2	20.0 ± 0.7	–	0.7 ± 0.1	31.3 ± 0.5	–	48.0 ± 0.6
Sample 3	8.9 ± 0.6	–	1.6 ± 0.1	18.5 ± 0.3	5.4 ± 0.2	65.6 ± 0.5

sample 3. Consequently, an additional phase containing binder elements should have formed in sample 3. Comparing the XRD patterns of all three samples, it is noticeable that a small peak is present only in sample 3 with a 2θ angle between 41° and 42°. This peak corresponds to the position of the most intense peak of the η-phases Ni_2W_4C, Co_2W_4C (ICCD 98-009-0811) or their mixed carbide $(Ni,Co)_2W_4C$ or simply M_2W_4C.[17] The formation of this additional η-phase could explain the lower content of the fcc α_{Co} binder phase and consequently, the lower toughness of such a material. One of the possible reasons for the formation of the additional η-phase could be related to the lower carbon content in the production process of WC-Co cemented-carbide tools.

4 CONCLUSIONS

Three different commercial WC-Co cemented-carbide tool materials, used as saw blades were characterized in this work, as one group exhibited a more frequent cracking.

The results of our work show that the binder phase in sample 3 contains a significant amount of nickel in addition to cobalt, while the other two samples do not. The results also show that despite having the same content of binder-forming elements in all three different commercial WC-Co carbide tools, the content of the binder phase in sample 3 is significantly lower. In addition, the size of the WC grains is also smaller in this sample. Both the binder content and the size of the WC grains lead to a decrease in the toughness of such a material, which results in the more frequent cracking of such tools. The results of this work also suggest that the cause of the lower content of the binder phase in sample 3 could be the formation of an additional η-phase of type M_2W_4C, which reduces the content of the fcc binder phase and thus the toughness.

Acknowledgements

5 REFERENCES

[1] J. García, V. Collado Ciprés, A. Blomqvist, B. Kaplan, Cemented carbide microstructures: a review, International Journal of Refractory Metals & Hard Materials, 80 (**2019**), 40–68, doi:10.1016/j.ijrmhm.2018.12.004

[2] A. T. Santhanam, Metallography of Cemented Carbides, Metallography and Microstructures, Vol. 9, ASM Handbook, ASM International, 2004, 1067–1078

[3] S. Norgren, J. García, A. Blomqvist, L. Yin, Trends in the P/M hard metal industry, International Journal of Refractory Metals and Hard Materials, 48 (**2015**), 31–45, doi:10.1016/j.ijrmhm.2014.07.007

[4] G. Gille, J. Bredthauer, B. Gries, B. Mende, W. Heinrich, Advanced and new grades of WC and binder powder – their properties and application, International Journal of Refractory Metals and Hard Materials, 18 (**2000**), 87–102, doi:10.1016/S0263-4368(00)00002-0

[5] B. Wittmann, W.-D. Schubert, B. Lux, WC grain growth and grain growth inhibition in nickel and iron binder hardmetals, International Journal of Refractory Metals and Hard Materials 20 (**2002**), 51–60, doi:10.1016/S0263-4368(01)00070-1

[6] H. Okamoto, Desk Handbook: Phase Diagrams for Binary Alloys, ASM International, 2000, 253

[7] J. M. Densley, J. P. Hirth, Fracture toughness of a nanoscale WC-Co tool steel, Scripta Materialia, 38 (**1998**), 239–244, doi:10.1016/S1359-6462(97)00435-1

[8] H. Saito, A. Iwabuchi, T. Shimizu, Effects of Co content and WC grain size on wear of WC cemented carbide, Wear, 261 (**2006**), 126–132, doi:10.1016/j.wear.2005.09.034

[9] A. V. Shatov, S. A. Firstov, I. V. Shatova, The shape of WC crystals in cemented carbides, Materials Science and Engineering A, 242 (**1998**), 7–14, doi:10.1016/S0921-5093(97)00509-1

[10] A. Delanoë, M. Bacia, E. Pauty, S. Lay, C. H. Allibert, Cr-rich layer at the WC/Co interface in Cr-doped WC–Co cermets: segregation or metastable carbide?, Journal of Crystal Growth, 270 (**2004**), 219–227, doi:10.1016/j.jcrysgro.2004.05.101

[11] S. Lay, J. Thibault, S. Hamar-Thibault, Structure and role of the interfacial layers in VC-rich WC-Co cermets, Philosophical Magazine, 83 (**2003**), 1175–1190, doi:10.1080/1478643031000075759

[12] S. A. E. Johansson, G. Wahnstr?m, A computational study of thin cubic carbide films in WC/Co interfaces, Acta Materialia, 59 (**2011**), 171–181, doi:10.1016/j.actamat.2010.09.021

[13] J. Weidow, H.-O. Andrén, Grain and phase boundary segregation in WC–Co with small V, Cr or Mn additions, Acta Materialia, 58 (**2010**), 3888–3894, doi:10.1016/j.actamat.2010.03.038

[14] G. Li, Y. Peng, L. Yan, T. Xu, J. Long, F. Luo, Effects of Cr concentration on the microstructure and properties of WC-Ni cemented carbides, Journal of Materials Research and Technology, 9 (**2020**), 902–907, doi:10.1016/j.jmrt.2019.11.030

[15] H. L. de Villiers Lovelock, Powder/processing/structure relationships in WC-Co thermal spray coatings: A review of the published literature, Journal of Thermal Spray Technology, 7 (**1998**), 357–373, doi:10.1361/105996398770350846

[16] J. Kim, Y. Jae Suh, I. Kang, First-principles calculations of the phase stability and the elastic and mechanical properties of η-phases in the WC-Co system, Journal of Alloys and Compounds, 656 (**2016**), 213–217, doi:10.1016/j.jallcom.2015.09.214

[17] V. B. Voitovich, V. V. Sverdel, R. F. Voitovich, E. I. Golovko, Oxidation of WC-Co, WC-Ni and WC-Co-Ni hard metals in the temperature range 500–800 °C, International Journal of Refractory Metals and Hard Materials, 14 (**1996**), 289–295, doi:10.1016/0263-4368(96)00009-1